JACS
JOURNAL OF THE AMERICAN CHEMICAL SOCIETY

COMMUNICATION

pubs.acs.org/JACS

The Role of Cobalt Phosphate in Enhancing the Photocatalytic Activity of α-Fe_2O_3 toward Water Oxidation

Monica Barroso,*[,†] Alexander J. Cowan,[†] Stephanie R. Pendlebury,[†] Michael Grätzel,[‡] David R. Klug,[†] and James R. Durrant*[,†]

[†]Department of Chemistry, Imperial College London, South Kensington Campus, London SW7 2AZ, United Kingdom

[‡]Institut des Sciences et Ingenierie Chimiques, Ecole Polytechnique Fédérale de Lausanne, CH-1015 Lausanne, Switzerland

Supporting Information

ABSTRACT: Transient absorption spectroscopy was used to probe the dynamics of photogenerated charge carriers in α-Fe_2O_3/CoO_x nanocomposite photoelectrodes for water splitting. The addition of cobalt-based electrocatalysts was observed to increase the lifetime of photogenerated holes in the photoelectrode by more than 3 orders of magnitude without the application of electrical bias. We therefore propose that the enhanced photoelectrochemical activity of the composite electrode for water photooxidation results, at least in part, from reduced recombination losses because of the formation of a Schottky-type heterojunction.

There is increasing interest in the use of solar energy to drive the photolysis of water into molecular hydrogen and oxygen by inorganic nanoparticles and photoelectrodes.[1−3] Nevertheless, despite decades of research, the quest for a single material with all of the characteristics required for unassisted solar water splitting has proved unsuccessful, and the reported solar-to-chemical energy conversion efficiencies are still too low to make these systems commercially viable. One strategy that can be used to enhance the photocatalytic activity of such materials is the addition of well-known water oxidation "cocatalysts", such as IrO_2, RuO_2, or Co_3O_4.[4] However, kinetic studies of the role of these cocatalysts have been relatively limited, and as a consequence, it is often unclear whether any enhanced activity results from specific catalytic function of the cocatalyst (i.e., by reducing activation energies for water oxidation) or by retardation of recombination kinetics. In this work, we employed transient absorption (TA) kinetic studies to address this issue for α-Fe_2O_3 (hematite) photoelectrodes coupled with cobalt-based oxygen-evolving catalysts (OECs), motivated in particular by the extensive interest these composite photoelectrodes are currently attracting for visible-light-driven water photooxidation.[5−8]

Hematite is a promising material for photoelectrochemical water splitting because of its stability, strong visible-light absorption, and favorable valence band position for water oxidation to O_2. However, water splitting with hematite photoanodes requires the application of a positive electrochemical bias, which is necessary both to retard electron/hole (e/h) recombination within the photoelectrode[9] and to increase the reduction potential of photogenerated electrons such that they are able to undertake the complementary water photoreduction reaction.[10] Several studies have shown that this requirement for electrochemical bias can be reduced by the coupling of cocatalysts, including Co^{2+},[11] cobalt phosphate (Co-Pi),[6] IrO_2,[12] and NiFe.[13]

Cobalt oxides and hydroxides have been extensively investigated for electrochemical water oxidation applications.[14−16] Recently, Co-Pi has been shown to be an effective electrocatalyst for oxygen evolution that can self-assemble onto electrode surfaces from phosphate-buffered solutions containing Co^{2+}.[17,18] Electrochemical,[19] XANES,[20] and EPR[21] analyses have indicated that the electrocatalytic function of Co-Pi is associated with oxidation from Co(II) to Co(III) and Co(IV) species, leading to the formation of high-valent Co(IV)−O intermediates.[19−21] The involvement of multiple cobalt oxidation states, the proposed molecular structure (an edge-sharing cubane dimer), and the capacity to self-regenerate have led to comparisons of this catalyst with the OEC of plant photosystem II.[18,22] The role played by phosphate is not fully understood, and other conjugated bases such as borate and methylphosphonate have been shown to support catalytic activity in a similar manner. Proton management, particularly at neutral pH, is possibly one of the functions of these electrolytes, but participation in the assembly of catalyst layers has also been suggested.[17,23,24] Co-Pi can also enhance the efficiency of water photooxidation when coupled with a range of metal oxide photoelectrodes, including ZnO,[5] WO_3,[7] and α-Fe_2O_3.[6,8] Photoelectrochemical studies of α-Fe_2O_3/Co-Pi photoelectrodes have indicated that this increased photoanode efficiency results from lower recombination losses,[6,8] most typically attributed to improved water oxidation kinetics,[8] although to date no direct studies of the kinetics of either recombination or oxidation processes have been reported for such composite photoelectrodes.

We recently used transient absorption spectroscopy (TAS) on the microsecond to second time scale with low excitation densities to show that the application of a positive electrochemical bias to nanostructured undoped hematite photoelectrodes can result in an increase in the lifetime of photogenerated holes from microseconds up to seconds.[9,25] We also reported analogous data for nanocrystalline TiO_2 photoelectrodes.[26] In both cases, the increase in hole lifetime was suggested to be essential to enable photogenerated holes to have sufficient time to drive the multielectron oxidation of water to molecular oxygen, which is particularly slow in α-Fe_2O_3.[27] In this work, we used TAS to investigate the effect of Co-based OECs, in particular Co-Pi, on the dynamics of charge carriers photogenerated in hematite thin-film electrodes.

For the studies reported herein, a three-electrode setup was used for the electrodeposition of Co-Pi on α-Fe_2O_3 working electrodes (α-Fe_2O_3/Co-Pi), employing a Pt mesh as the

Received: June 20, 2011
Published: August 23, 2011

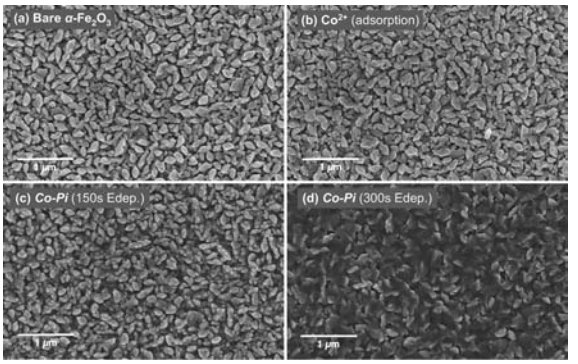

Figure 1. SEM micrographs comparing the surface of a bare Nb-doped mesoporous hematite film (a) before and (b) after Co^{2+} treatment. The effect of electrodeposition of Co-Pi for (c) 150 and (d) 300 s is also shown, revealing homogeneous coverage of the hematite film surface.

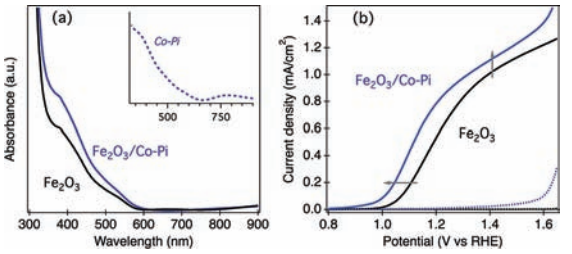

Figure 2. Effect of Co-Pi on the optical and photoelectrochemical properties of iron oxide photoelectrodes. (a) UV−vis absorption spectra of an α-Fe_2O_3 photoanode without (black) and with (blue) cocatalyst (300 s electrodeposition). The inset shows the difference spectrum, which corresponds to the optical absorption by Co-Pi. (b) Dark-current (dashed) and photocurrent (solid) densities measured in 0.1 M NaOH (pH 12.6) before (black) and after (blue) Co-Pi electrodeposition.

counter electrode and Ag/AgCl/3 M NaCl as the reference electrode. The electrolyte solution contained 0.5 mM cobalt nitrate in a 0.1 M potassium phosphate (KPi) buffer adjusted to pH 7, as described elsewhere for the preparation of similar composite photoanodes.[18,28] Deposition times of up to 300 s at +1.0 V vs Ag/AgCl produced thin layers of the cocatalyst, which could be detected by scanning electron microscopy (SEM) and UV−vis absorption spectroscopy (Figures 1 and 2a, respectively). The data reported in this paper were obtained using mesoporous Nb-doped α-Fe_2O_3 films with thicknesses of 150−200 nm that were fabricated by ultrasonic spray pyrolysis (USP)[29] on fluorine-doped tin oxide (FTO) glass [further experimental details are given in the Supporting Information (SI)], as their high homogeneity and low optical scattering facilitated the TAS measurements. Relatively thin cocatalyst layers were chosen for our studies to enable high optical transparency of the composite electrodes and minimize the filtering effect from unproductive light absorption by Co-Pi.[30] Simple adsorption of Co^{2+} ions onto the surface of hematite (hereafter designated Co^{2+} treatment) is known to enhance the efficiency of photoelectrochemical water oxidation in a manner similar to Co-Pi.[6,11] For this reason, we also investigated the charge-carrier dynamics in α-Fe_2O_3/Co^{2+} electrodes. The Co^{2+} treatment was performed by dipping the hematite electrode in aqueous 0.5 mM $Co(NO_3)_2$ for 2 h followed by rinsing with deionized water. We note that the effects of Co-Pi were found to be retained for several days while those of Co^{2+} tended to diminish during prolonged measurements, although they could be recovered by repeating the treatment.

The optical absorption spectra of bare and composite photoelectrodes are shown in Figure 2a. The contribution from Co-Pi (Figure 2a inset), which was obtained from the difference between the spectra of the bare α-Fe_2O_3 and composite α-Fe_2O_3/Co-Pi electrodes, shows a strong absorption band extending to 600 nm with a maximum at ∼380 nm and a weaker absorption in the region 700−900 nm. These bands are assigned to the absorption of Co(II) and Co(III) species, in agreement with literature reports.[31]

Figure 2b shows the current−voltage responses of bare and Co-Pi-coated α-Fe_2O_3 photoanodes measured in 0.1 M NaOH (12.8) in a three-electrode cell with a Pt mesh counter electrode and Ag/AgCl/3 M NaCl reference electrode when the film was illuminated from the electrolyte−electrode (EE) side with 1 sun (100 mW cm^{-2}, AM 1.5G) simulated sunlight. The reported potentials are versus the reversible hydrogen electrode (RHE) and were obtained using the Nernst equation, $E_{RHE} = E_{Ag/AgCl} + 0.0591 \cdot pH + 0.21$. The electrodeposition of Co-Pi produced a >100 mV cathodic shift of the photocurrent onset potential and an increase in the saturation photocurrent (100 $\mu A/cm^2$ at 1.4 V vs RHE), in agreement with observations by other groups using similar composite electrodes.[6,8,28] It should be noted that the magnitude of the Co-Pi effect was dependent on the nanomorphology and photocurrent performance of the bare electrode as well as the time and method of Co-Pi deposition.

TA spectra of bare α-Fe_2O_3 and composite α-Fe_2O_3/Co-Pi electrodes are compared in Figures 3a,b. Figure 4 shows the corresponding kinetics at two probe wavelengths (580 and 900 nm). These measurements were performed using UV laser excitation (355 nm, 0.33 Hz, EE side) at low excitation density (0.2 mJ/cm^2) in a sealed quartz cuvette where the electrodes were immersed in Ar-purged KPi electrolyte without electrical bias.

For both films, at early times a broad positive absorption was observed across the wavelength range probed; this was assigned to the absorption of photogenerated hematite holes. Support for this assignment came primarily from our observation that the amplitude and lifetime of this broad photoinduced absorption increased under positive anodic biases (Figure S1 in the SI), conditions expected to result in electron extraction from the film and therefore enhanced hole yields and lifetimes, as we have discussed previously.[9,24] In addition to this broad photoinduced absorption, more complex spectroscopic and kinetic behavior was observed in the region around 580 nm. As we discuss below, this ∼580 nm feature was assigned primarily to absorption of a specific intraband trap state.

The most striking effect of the Co-Pi treatment upon the TA data is a dramatic retardation of the decay dynamics. This is most easily observed from the TA decays shown at 900 nm in Figure 4, corresponding to the absorption of hematite holes. For the bare α-Fe_2O_3 electrodes (Figure 4a), a relatively fast (microsecond) power-law decay was observed, analogous to those we reported previously for APCVD-deposited films[9] and assigned to bimolecular recombination of photogenerated electrons and holes. As we have discussed previously, this rapid recombination dynamics is fast in comparison with water oxidation by photogenerated holes on hematite photoanodes (which occurs on a time scale of seconds),[9,25,32] consistent with the observed negligible water oxidation on such photoelectrodes without the application of a positive electrical bias. Figure 4b shows the corresponding TA decay for the α-Fe_2O_3/Co-Pi composite. It is striking that the addition of Co-Pi dramatically increased the lifetime of the

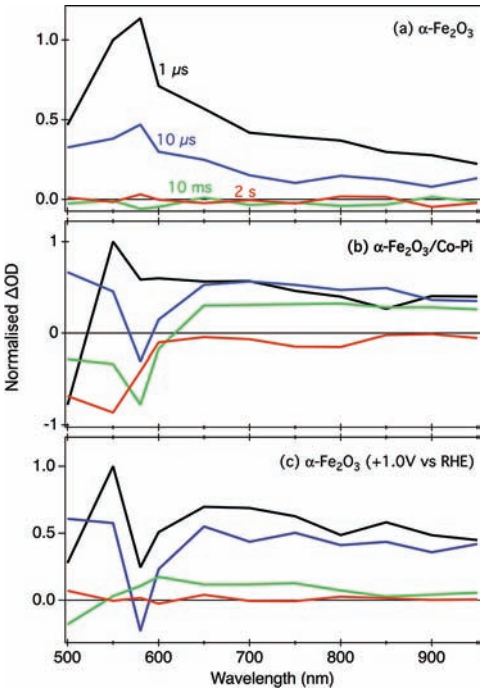

Figure 3. TA spectra of bare and Co-Pi-treated Nb-doped USP α-Fe_2O_3 electrodes measured at 1 μs (black), 10 μs (blue), 10 ms (green), and 2s (red) after UV laser excitation (355 nm, 200 μJ/cm^2, 0.33 Hz, EE side): (a) isolated bare electrode; (b) isolated composite electrode; (c) bare electrode held at +1.0 V vs RHE in Ar-purged KPi buffer (pH 7). The TA difference (ΔOD) was normalized at 550 nm, 1 μs.

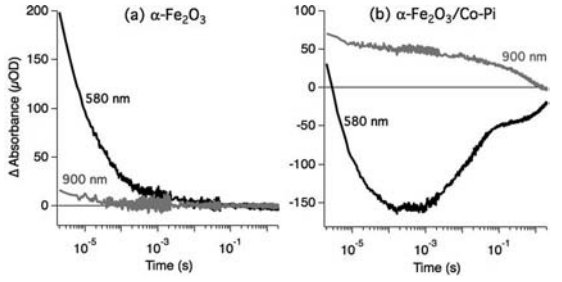

Figure 4. TA decays of Nb-doped USP α-Fe_2O_3 (a) before and (b) after 300 s electrodeposition of Co-Pi. Decay traces were recorded after UV laser excitation (355 nm, 200 μJ/cm^2, 0.33 Hz) and probed at 580 and 900 nm, within the absorption band of α-Fe_2O_3 photoholes. All measurements were performed on isolated films in 0.1 M KPi buffer (pH 7) under EE illumination.

transient by more than 3 orders of magnitude, with $t_{1/2}$ increasing from ~15 μs in the bare film to ~30 ms in the composite. This increase is of similar magnitude to that observed previously for bare α-Fe_2O_3 electrodes under the application of positive electrochemical bias, with absorption transients exhibiting lifetimes in the order of seconds[25] (Figure S1), and clearly indicates that the deposition of Co-Pi results in a substantial retardation of e/h recombination relative to the bare α-Fe_2O_3 film.

In addition to the clear increase in charge-carrier lifetime resulting from the addition of Co-Pi, the transient data for the composite α-Fe_2O_3/Co-Pi films showed more complex kinetic behavior than that observed for the bare α-Fe_2O_3 films, particularly between 500 and 600 nm. Most obviously, a positive TA band observed at ~580 nm for bare α-Fe_2O_3 was inverted to a negative feature for α-Fe_2O_3/Co-Pi. In our previous studies with undoped α-Fe_2O_3, we ascribed the positive signal at 580 nm to the absorption of surface-trapped photoholes generated after optical excitation, which agrees well with the suggestion that holes trapped as Fe^{4+} in iron-doped perovskites and rutile are responsible for optical absorption bands with maxima at 2.1 eV[33,34] and the generally accepted predominance of Fe(IV) character for the holes in hematite.[27] Following this assignment, we tentatively assign the bleaching feature observed after Co-Pi treatment to photoinduced reduction of such surface-trapped holes. This assignment is supported by our observation that the TA spectra of hematite films biased anodically also revealed a bleaching centered at 580 nm accompanying the longer lifetime observed in the region 650−950 nm (Figure 3c), very similar to that observed following Co-Pi treatment in the absence of applied bias. This suggests that the 580 nm feature likely corresponds to a particular set of intraband states that can function as either hole or electron traps, depending upon their initial redox state as determined by the electrode potential and/or surface treatment. Passivation effects of surface trap states have recently been reported for α-Fe_2O_3 surfaces treated with Al^{3+} or Sn^{4+} [35] or coated with Al_2O_3[36] or other group-13 oxide overlayers.[37] Further studies are underway to identify more thoroughly the chemical nature of the 580 nm signal and its impact upon the photoelectrochemical performance of these films.

For the composite film, there was a further evolution of the TA on the 100 ms time scale, resulting in the TA spectrum at 2 s (red trace in Figure 3b). This spectrum exhibits no photoinduced absorption but does show clear bleach signals at 500−600 and 700−850 nm. This long-time-scale bleach was observed mostly when thicker layers of Co-Pi were produced (with longer electrodeposition times) but was also seen for films treated with Co^{2+}. However, no obvious correlation between the magnitude of this long-time-scale bleach and the photoelectrochemical response of the composite electrodes was found. Cobalt oxides and oxyhydroxides are known to exhibit electrochromism, changing from light-yellow to opaque (gray) upon oxidation from Co(II) to Co(III) states.[38] Therefore, we tentatively assign the long-time-scale bleach to a loss of the characteristic optical absorption of Co(III) species. The mechanism through which this bleach is formed and subsequently decays is, however, not fully understood and requires further investigation.

Scheme 1 illustrates the conclusions of our transient kinetic studies in terms of the charge-carrier dynamics in α-Fe_2O_3 and α-Fe_2O_3/CoO_x films, where CoO_x represents the cobalt oxo/hydroxo[20] layer resulting from Co-Pi electrodeposition or other similar Co-based treatments. In bare hematite, photogenerated electrons and holes recombine rapidly on the microsecond time scale. However, for the α-Fe_2O_3/CoO_x films, this recombination is retarded by at least 3 orders of magnitude. This retardation of e/h recombination within α-Fe_2O_3 resulting from CoO_x deposition appears to occur without requiring hole transfer to the CoO_x layer, as most obviously indicated by the similarity of the TA spectra observed for the Fe_2O_3/Co-Pi film without anodic bias and bare Fe_2O_3 under anodic bias (Figure 3a,c; also see the SI). This retardation therefore most probably cannot be ascribed to spatial separation of electrons and holes across the Fe_2O_3/CoO_x interface. Rather, it appears that addition of the Co-based layer results in a dramatic retardation of e/h recombination within the α-Fe_2O_3 element of the composite photoelectrode, analogous to that observed when a small positive electrical bias is applied. A possible explanation for this effect could be the formation of an α-Fe_2O_3/CoO_x heterojunction that corresponds to depletion of

Scheme 1. Schematic Band Diagrams Illustrating the Main Fates of Photogenerated Charge Carriers following Light Excitation in (a) Bare α-Fe_2O_3 and (b) Composite α-Fe_2O_3/CoO_x in Contact with KPi Electrolyte at pH 7

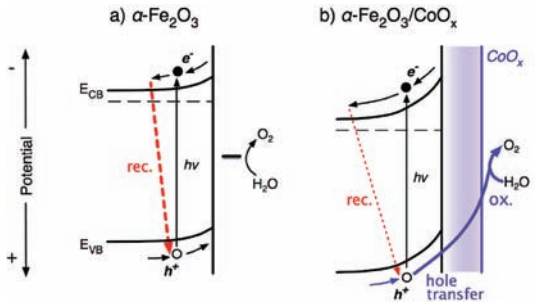

electrons in the Fe_2O_3 conduction band, most probably resulting in increased band bending in the α-Fe_2O_3, as illustrated in Scheme 1. This band bending contributes to the separation of electrons and holes within the α-Fe_2O_3 film, reducing the density of electrons adjacent to the α-Fe_2O_3/CoO_x interface. Similar Schottky-type heterojunctions have been suggested to be responsible for enhanced charge separation in composite photoanodes, as in the case of $BiVO_4$/Co_3O_4.[39] The band-bending enhancement is also consistent with the oxidative nature of cobalt treatments and suggests that the resultant surface depletion of Fe_2O_3 electrons is retained even after the formation of the cobalt oxide layer is completed.

In summary, we conclude that cobalt oxide overlayers such as Co-Pi increase the lifetime of photogenerated holes in hematite photoanodes. We have demonstrated that deposition of Co-Pi on α-Fe_2O_3 results in a retardation of the kinetics of e/h recombination by at least 3 orders of magnitude. This retardation is consistent with the smaller anodic potential required for the onset of photocurrent generation in such composite photoelectrodes. Thus, it appears likely that the enhanced water photooxidation properties of α-Fe_2O_3/Co-Pi and in general α-Fe_2O_3/CoO_x composite photoanodes result significantly from retardation of e/h recombination due to the formation of an inorganic heterojunction and enhanced charge separation.

■ ASSOCIATED CONTENT

Supporting Information. Full experimental details and additional TAS results. This material is available free of charge via the Internet at http://pubs.acs.org.

■ AUTHOR INFORMATION

Corresponding Author
m.barroso@imperial.ac.uk; j.durrant@imperial.ac.uk

■ ACKNOWLEDGMENT

Financial support from the EPSRC is gratefully acknowledged, as are helpful discussions and initial results from Frederico Sanches and Dr. Stephen Dennison. We also thank Dr. Christopher Barnett for equipment development and maintenance.

■ REFERENCES

(1) Maeda, K.; Domen, K. *J. Phys. Chem. Lett.* **2010**, *1*, 2655.
(2) Kudo, A.; Miseki, Y. *Chem. Soc. Rev.* **2009**, *38*, 253.
(3) Osterloh, F. E. *Chem. Mater.* **2008**, *20*, 35.
(4) Harriman, A.; Pickering, I. J.; Thomas, J. M.; Christensen, P. A. *J. Chem. Soc., Faraday Trans. 1* **1988**, *84*, 2795.
(5) Steinmiller, E. M. P.; Choi, K. S. *Proc. Natl. Acad. Sci. U.S.A.* **2009**, *106*, 20633.
(6) Zhong, D. K.; Cornuz, M.; Sivula, K.; Grätzel, M.; Gamelin, D. R. *Energy Environ. Sci.* **2011**, *4*, 1759.
(7) Seabold, J. A.; Choi, K.-S. *Chem. Mater.* **2011**, *23*, 1105.
(8) McDonald, K. J.; Choi, K.-S. *Chem. Mater.* **2011**, *23*, 1686.
(9) Pendlebury, S. R.; Barroso, M.; Cowan, A. J.; Sivula, K.; Tang, J.; Grätzel, M.; Klug, D.; Durrant, J. R. *Chem. Commun.* **2011**, *47*, 716.
(10) Sivula, K.; Le Formal, F.; Grätzel, M. *ChemSusChem* **2011**, *4*, 432.
(11) Kay, A.; Cesar, I.; Grätzel, M. *J. Am. Chem. Soc.* **2006**, *128*, 15714.
(12) Tilley, S. D.; Cornuz, M.; Sivula, K.; Grätzel, M. *Angew. Chem., Int. Ed.* **2010**, *49*, 6405.
(13) Kleiman-Shwarsctein, A.; Hu, Y.-S.; Stucky, G. D.; McFarland, E. W. *Electrochem. Commun.* **2009**, *11*, 1150.
(14) Elizarova, G. L.; Zhidomirov, G. M.; Parmon, V. N. *Catal. Today* **2000**, *58*, 71.
(15) Frei, H.; Jiao, F. *Angew. Chem., Int. Ed.* **2009**, *48*, 1841.
(16) Artero, V.; Chavarot-Kerlidou, M.; Fontecave, M. *Angew. Chem., Int. Ed.* **2011**, *50*, 7238.
(17) Surendranath, Y.; Dincă, M.; Nocera, D. G. *J. Am. Chem. Soc.* **2009**, *131*, 2615.
(18) Kanan, M. W.; Surendranath, Y.; Nocera, D. G. *Chem. Soc. Rev.* **2009**, *38*, 109.
(19) Surendranath, Y.; Kanan, M. W.; Nocera, D. G. *J. Am. Chem. Soc.* **2010**, *132*, 16501.
(20) Kanan, M. W.; Yano, J.; Surendranath, Y.; Dincă, M.; Yachandra, V. K.; Nocera, D. G. *J. Am. Chem. Soc.* **2010**, *132*, 13692.
(21) McAlpin, J. G.; Surendranath, Y.; Dincă, M.; Stich, T. A.; Stoian, S. A.; Casey, W. H.; Nocera, D. G.; Britt, R. D. *J. Am. Chem. Soc.* **2010**, *132*, 6882.
(22) Risch, M.; Khare, V.; Zaharieva, I.; Gerencser, L.; Chernev, P.; Dau, H. *J. Am. Chem. Soc.* **2009**, *131*, 6936.
(23) Symes, M. D.; Surendranath, Y.; Lutterman, D. A.; Nocera, D. G. *J. Am. Chem. Soc.* **2011**, *133*, 5174.
(24) Esswein, A. J.; Surendranath, Y.; Reece, S. Y.; Nocera, D. G. *Energy Environ. Sci.* **2011**, *4*, 499.
(25) Cowan, A. J.; Barnett, C. J.; Pendlebury, S. R.; Barroso, M.; Sivula, K.; Grätzel, M.; Durrant, J. R.; Klug, D. R. *J. Am. Chem. Soc.* **2011**, *133*, 10134.
(26) Cowan, A. J.; Tang, J. W.; Leng, W. H.; Durrant, J. R.; Klug, D. R. *J. Phys. Chem. C* **2010**, *114*, 4208.
(27) Dare-Edwards, M. P.; Goodenough, J. B.; Hamnett, A.; Trevellick, P. R. *J. Chem. Soc., Faraday Trans. 1* **1983**, *79*, 2027.
(28) Zhong, D. K.; Gamelin, D. R. *J. Am. Chem. Soc.* **2010**, *132*, 4202.
(29) Duret, A.; Grätzel, M. *J. Phys. Chem. B* **2005**, *109*, 17184.
(30) Zhong, D. K.; Sun, J. W.; Inumaru, H.; Gamelin, D. R. *J. Am. Chem. Soc.* **2009**, *131*, 6086.
(31) Lenglet, M.; Jorgensen, C. K. *Chem. Phys. Lett.* **1994**, *229*, 616.
(32) Wijayantha, K. G. U.; Saremi-Yarahmadi, S.; Peter, L. M. *Phys. Chem. Chem. Phys.* **2011**, *13*, 5264.
(33) Faughnan, B. W.; Kiss, Z. J. *Phys. Rev. Lett.* **1968**, *21*, 1331.
(34) Nozik, A. J. *J. Phys. C: Solid State Phys.* **1972**, *5*, 3147.
(35) Spray, R. L.; McDonald, K. J.; Choi, K.-S. *J. Phys. Chem. C* **2011**, *115*, 3497.
(36) Le Formal, F.; Tetreault, N.; Cornuz, M.; Moehl, T.; Grätzel, M.; Sivula, K. *Chem. Sci.* **2011**, *2*, 737.
(37) Hisatomi, T.; Le Formal, F.; Cornuz, M.; Brillet, J.; Tetreault, N.; Sivula, K.; Grätzel, M. *Energy Environ. Sci.* **2011**, *4*, 2512.
(38) Da Fonseca, C. N. P.; Depaoli, M. A.; Gorenstein, A. *Sol. Energy Mater. Sol. Cells* **1994**, *33*, 73.
(39) Kisch, H.; Long, M. C.; Cai, W. M. *J. Phys. Chem. C* **2008**, *112*, 548.